

Three-dimensional structure of a halotolerant algal carbonic anhydrase predicts halotolerance of a mammalian homolog

Lakshmanane Premkumar^{*†}, Harry M. Greenblatt[†], Umesh K. Bageshwar^{*}, Tatyana Savchenko^{*}, Irena Gokhman^{*}, Joel L. Sussman^{†‡}, and Ada Zamir^{**}

Departments of ^{*}Biological Chemistry and [†]Structural Biology, Weizmann Institute of Science, Rehovot 76100, Israel

Communicated by Ada Yonath, Weizmann Institute of Science, Rehovot, Israel, April 6, 2005 (received for review December 27, 2004)

Protein molecular adaptation to drastically shifting salinities was studied in dCA II, an α -type carbonic anhydrase (EC 4.2.1.1) from the exceptionally salt-tolerant unicellular green alga *Dunaliella salina*. The salt-inducible, extracellular dCA II is highly salt-tolerant and thus differs from its mesophilic homologs. The crystal structure of dCA II, determined at 1.86-Å resolution, is globally similar to other α -type carbonic anhydrases except for two extended α -helices and an added Na-binding loop. Its unusual electrostatic properties include a uniformly negative surface electrostatic potential of lower magnitude than that observed in the highly acidic halophilic proteins and an exceptionally low positive potential at a site adjoining the catalytic Zn²⁺ compared with mesophilic homologs. The halotolerant dCA II also differs from typical halophilic proteins in retaining conformational stability and solubility in low to high salt concentrations. The crucial role of electrostatic features in dCA II halotolerance is strongly supported by the ability to predict the unanticipated halotolerance of the murine CA XIV isozyme, which was confirmed biochemically. A proposal for the functional significance of the halotolerance of CA XIV in the kidney is presented.

nonhalophilic | protein salt adaptation | x-ray structure

Life in extreme or radically varying environments entails the molecular adaptation of cellular constituents, primarily proteins, as safeguards against structural and functional damage. Comparative structure–function studies of homologous proteins of mesophilic, extremophilic, or extremotolerant origins unravel molecular strategies underlying the astounding acclimation power of proteins. Molecular adaptation of proteins to salt is of particular interest considering the influence of salt on protein folding, oligomerization, solubility, and function (1). Most mesophilic proteins function optimally at relatively low salinities and are adversely affected at high salinities. However, proteins from extremely halophilic archaea, living in hypersaline environments, typically require 1–2 M KCl or NaCl for proper folding and activity (1, 2). Halophilic proteins are characterized by a high negative surface electrostatic potential primarily due to the high abundance of surface acidic residues (1–6). Halophilic adaptation is best explained by the solvation–stabilization model whereby surface acidic residues bind hydrated ions to form a solvation shell that prevents water or salt enrichment at the protein surface, thus allowing the proteins to remain soluble and properly folded at high salt (1, 7, 8). These solvent–protein interactions are greatly dependent on the nature of the solvent salts (7, 8). Complex salt bridge networks, weak protein–protein interactions, and specific ion-binding were identified as additional elements enhancing the stability and solubility of the model halophilic protein, malate dehydrogenase from *Haloarcula marismortui* (3, 7–10).

A different response to salt is displayed by a versatile group of halotolerant proteins, mainly from nonhalophilic as well as halophilic microbial sources that remain active throughout a

broad range of salinities without exhibiting obligatory salt dependence (11–16). The structural principles discriminating halotolerant from mesophilic and halophilic proteins have yet to be elucidated. A valuable source of such proteins is the unicellular green alga *Dunaliella salina* that proliferates in low to nearly saturating salt concentrations while attaining osmotic balance by intracellular accumulation of glycerol (17). Consequently, the algal extracellular proteins should be able to cope with the extremely broad spectrum of salinities sustaining algal growth. Two extracellular proteins identified in our studies that conform to this expectation are dCA I, a 60-kDa protein consisting of two \approx 52% identical, repeated α -type carbonic anhydrase (CA) domains (18), and the more recently discovered dCA II, an \approx 30-kDa, single-domain CA exhibiting \approx 55% sequence identity to each of the dCA I domains (19).

The CAs, found predominantly in animals but also in bacteria and green algae, catalyze the reversible hydration of CO₂ to form bicarbonate and a proton. The catalytic mechanism employs a Zn-bound hydroxide in the active site as a nucleophile in CO₂ hydration to bicarbonate, a step followed by the regeneration of the Zn-bound hydroxide by intermolecular proton transfer via a shuttling amino acid residue(s) from the Zn-bound water to a buffer molecule (20). An important corollary of this mechanism is the inhibition of these enzymes by various monovalent anions, including Cl[−] and Br[−], that displace the catalytically essential Zn-bound water/hydroxyl and disrupt hydrogen-bonded networks at the active site, as indicated in crystal structures of CA-anion adducts (21, 22).

The results presented here for dCA II provide insights into the structural and electrostatic features that make a CA functionally halotolerant. The lessons learned from the structure of the algal CA allowed us to predict and confirm the unexpected halotolerance of a membrane-associated mammalian homolog of vital importance in renal function.

Materials and Methods

Enzyme Assays. Assays of affinity-purified dCA II (19), hCA I (Sigma), or mCA XIV (kindly provided by W. S. Sly, Saint Louis University, St. Louis) for bicarbonate dehydration and esterase activities were performed as described in refs. 18 and 23. CO₂ hydration activity was assayed at 22°C essentially as reported in refs. 18 and 23 with the following modifications: the reaction mixtures contained 25 mM Tris-sulfate buffer (pH 8.0) and the indicated concentrations of NaCl. The reaction was initiated by

Freely available online through the PNAS open access option.

Abbreviations: CA, α -type carbonic anhydrase; CR, conserved region; VR, variable region; VCR, variable conserved region.

Data deposition: The atomic coordinates and structure factors have been deposited in the Protein Data Bank, www.pdb.org (PDB ID code 1Y7W).

[†]To whom correspondence may be addressed. E-mail: joel.sussman@weizmann.ac.il or ada.zamir@weizmann.ac.il.

© 2005 by The National Academy of Sciences of the USA

the addition of 1.2 ml of CO₂-saturated water and monitored with a temperature-compensated pH meter interfaced to a personal computer. The initial rate was calculated from the linear part of the pH change corrected by subtraction of the rate of the uncatalyzed reaction.

Structure Determination and Refinement. Crystals of recombinant dCA II were obtained by using the vapor diffusion method (19). The crystals were cryoprotected with paraffin oil. Native data were collected in-house at 120 K by using R-AXIS IV⁺⁺ to 1.86-Å resolution. For phasing, multiwavelength anomalous dispersion data sets were collected at 100 K at three wavelengths around the zinc absorption edge on beamline BM14 at the European Synchrotron Radiation Facility. Diffraction data were processed with DENZO and SCALEPACK (24). Zinc positions were located on the basis of the anomalous difference. Experimental phases, to 2.0-Å resolution, were calculated from the multiwavelength anomalous dispersion data by using CNS (25), resulting in an overall figure of merit of 0.539. Phases were improved by applying solvent-flipping density modification using CNS, resulting in an overall figure of merit of 0.942. Based on the experimental map, 92% of the initial model was built by using XTALVIEW (26). A rigid body refinement in CNS using the initial model and native amplitudes extended the resolution to 1.86 Å. Further refinement and model building was carried out in CNS and XTALVIEW, respectively. The data collection and refinement statistics are given in Table 5, which is published as supporting information on the PNAS web site.

Structural Analysis, Numerical Calculations, and Comparisons. The following coordinate sets were obtained from the Protein Data Bank (www.pdb.org): ID codes 1JCZ (human carbonic anhydrase XII, hCA XII), 2CBA (human carbonic anhydrase I, hCA I), 1ZNC (human carbonic anhydrase IV, hCA IV), 1KOQ (*Neisseria gonorrhoeae* carbonic anhydrase, nCA), 1RAZ (human carbonic anhydrase II, hCA II), 1V9E (bovine carbonic anhydrase II, bCA II), 1RJ5 (murine carbonic anhydrase XIV, mCA XIV). The contents of secondary structure elements were calculated by DSSP (27). Surface accessibility was assessed by DSSP using a per-residue cut-off of 25 Å², with a probe radius of 1.4 Å. Structure-based sequence alignments were carried out by using LSQMAN (28) and/or SWISSPDBVIEWER (29). Determination of conserved regions (CRs), variable regions (VRs), and variable conserved regions (VCRs) used a 2.7-Å cut-off criterion. Molecular figures were generated in PYMOL (http://pymol.org), and the surface electrostatic figures were generated in GRASP (30). The electrostatic potential calculations were performed by using DELPHI software (31).

Additional information related to materials and methods including details of electrostatic calculations can be found in *Supporting Text*, which is published as supporting information on the PNAS web site.

Results

Localization, Induction, and Enzymatic Activity of dCA II. The extracellular localization of dCA II in *D. salina* and its induction in response to increasing salinities or depletion of bicarbonate resembled those reported in refs. 32 and 33 for dCA I. The detailed results are presented in *Supporting Text* and also in Fig. 4, which is published as supporting information on the PNAS web site.

The salt tolerance of dCA II was demonstrated in assays of three different CA activities. The steady-state kinetic measurements of bicarbonate dehydration, determined at pH 6.8, indicated that k_{enz} and K_m remained nearly constant in up to 0.5 M NaCl (Table 1). Assays performed at acidic pH indicated that the IC₅₀ for NaCl remained >0.5 M even at pH 5.6 (data not shown). The k_{enz} for esterase activity rose continuously with salt con-

Table 1. Effect of salt on the kinetic parameters of bicarbonate dehydration activity of dCA II

[NaCl], M	K_m , * mM	k_{cat} , * (ms) ⁻¹	k_{enz} , (M·μs) ⁻¹
dCA II			
0	28.7 ± 3.0	38.3 ± 1.5	1.33
0.1	30.1 ± 4.5	44.6 ± 2.5	1.48
0.25	32.2 ± 7.9	41.2 ± 4.0	1.27
0.5	33.4 ± 12.4	39.1 ± 5.9	1.17
hCA I			
0	19.7 ± 2.5	29.5 ± 1.3	1.50
0.1	80.1 ± 11.4	28.7 ± 2.3	0.36

Steady-state kinetics parameters were determined essentially as described in ref. 18. Assay mixtures contained the indicated concentrations of NaCl and 0.28 μM hCA I or 0.54 μM dCA II.

*Values are ± SE.

centration, reaching an ≈2-fold increase at 2.0 M NaCl relative to the activity in the absence of salt (Table 2). CO₂ hydration assays indicated that the enzyme retained activity to at least 1.5 M NaCl (described below). Although measurements at higher salinities were constrained by the interference of salt in the assay, dCA II activity was detectable even at 4.0 M NaCl. Similar responses to salt were observed in assays of dCA I (18). In contrast, a representative mesophilic homolog, hCA I, was strongly inhibited already at 0.1 M NaCl. Specifically, at this salt concentration, the K_m for bicarbonate increased ≈4-fold (Table 1), whereas the efficiency of esterase activity dropped by 75% (Table 2) relative to the activity in the absence of salt. The exceptional halotolerance of dCA I and dCA II is further demonstrated in a comparison with eight additional mesophilic CAs for Cl⁻ inhibition constants (see Table 6, which is published as supporting information on the PNAS web site).

Overall Structure of dCA II. The x-ray structure of dCA II was determined at 1.86-Å resolution (R factor, 16.7%; R_{free} , 20.2%). The asymmetric unit of the crystal contains two dCA II molecules, Mol A and Mol B, related by noncrystallographic symmetry with a root-mean-square (rms) deviation of 0.25 Å for the C^α atoms. The global fold of dCA II resembles that of other CAs in its central antiparallel 10-stranded β-sheet, two α-helices, and the presence of a catalytic Zn²⁺ (Fig. 1). This similarity is exemplified by the structure-based sequence alignment of dCA II (274 aa) with the best-characterized human isozyme, hCA II (259 aa), which shows 24% sequence identity and a rms deviation of 1.4 Å for 176 C^α atoms. Like other membrane-attached CAs (34, 35), dCA II contains a single disulfide linkage between

Table 2. Effect of salt on the kinetic parameters of dCA II esterase activity

[NaCl], M	k_{enz} , * (M·s) ⁻¹	k_{enz} , % of control
dCA II		
0.0	66.2 ± 1.0	100
0.1	88.0 ± 2.3	133
0.4	91.0 ± 2.0	138
1.0	102.0 ± 1.0	155
2.0	121.0 ± 2.1	183
hCA I		
0.0	498.0 ± 7.5	100
0.1	120.0 ± 2.1	24

Enzymatic assays for esterase activity were performed essentially as described in ref. 18. Assay mixtures contained the indicated concentrations of NaCl and 0.54 μM hCA I or 3.37 μM dCA II.

*Values are ± SE.

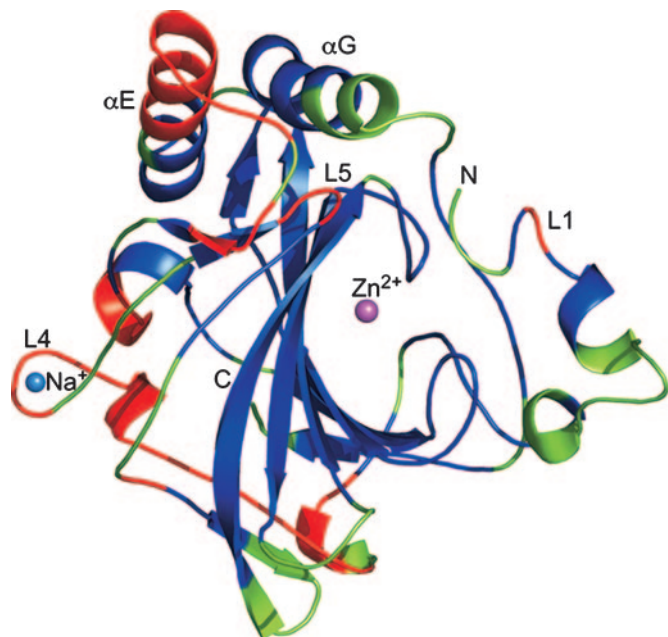


Fig. 1. Ribbon diagram of the dCA II structure. The regions corresponding to CRs (blue), VRs (green), and VCRs (red), as defined in the text, are mapped onto the dCA II structure. Marked are the catalytic Zn^{2+} and insertions and deletions in VCRs including L1 (the Zn binding loop), L4 (the Na-binding loop), and L5 as well as the two extended α -helices (E and G). N and C termini are indicated.

Cys-31 and Cys-221 (equivalent to Cys-23 and Cys-201 in hCA XII).

To identify structural features unique for dCA II, its structure was compared with seven mammalian and one bacterial CA structures deposited in the Protein Data Bank. In these eight structures, fully conserved structural elements, referred to as CRs, were identified by pairwise structural alignments of C^α atoms, ignoring whether the sequences are similar or not. The remaining, structurally variable regions located mostly within surface loops are referred to as VRs. Although most CRs are conserved in the dCA II structure, some CRs, designated as VCRs, have undergone significant modifications and thus may be specific for dCA II. The mapping of VR, CR, and VCR sections on the dCA II structure (Fig. 1) shows VCRs that differ from corresponding CRs by sequence deletions, insertions, and amino acid replacements. The deletion in the VCR corresponding to L5 creates a kink at the position occupied by the proton-shuttling His-64 in highly efficient CAs, which is not present in dCA II. The insertion in the VCR corresponding to α E and the restructuring of a VR contiguous with α G extend these two helices in dCA II with respect to the other CAs included in the comparison. Specifically, in dCA II α E contains 15 aa (Ala-166 to Asp-181), and α G is 14 aa (Arg-238 to Ala-251), as compared with hCA II where α E is 6 aa (Gly-156 to Val-161) and α G is 7 aa (Ser-220 to Phe-226) long. A quantitative comparison of secondary structure elements (see Table 7, which is published as supporting information on the PNAS web site) indicates that dCA II is significantly more enriched in helical content, moderately poorer in β -strand structures, and similar in the proportion of loops and turns relative to other CAs.

Other VCRs include the insertions that form loops L1 and L4 that bind a noncatalytic Zn^{2+} and a Na^+ , respectively (Fig. 1). The identification of the bound Na^+ was based on the observed octahedral coordination geometry and ligand distances (36) as shown in Fig. 5a, which is published as supporting information on the PNAS web site. The bound Na^+ presumably originated in

Table 3. Comparison of amino acid distribution in solvent accessible surface area

CAs	Polar, %	Nonpolar, %	Acidic, %	Basic, %	Acidic/basic ratio
dCA II	47.6	22.1	21.4	8.9	2.4
hCA XII	43.7	25.7	17.9	12.7	1.4
hCA II	34.5	19.3	21.9	24.2	0.9
nCA	39.6	21.0	14.9	24.6	0.6
hCA IV	33.4	22.4	18.0	26.2	0.7
hCA I	39.7	21.6	18.2	20.4	0.9
mCA V	33.4	24.6	22.1	19.8	1.1
bCA II	33.5	24.8	20.7	21.0	1.0

Calculations were performed as described in *Materials and Methods*. Polar: Asn, Gln, His, Ser, Thr, Tyr; nonpolar: Ala, Gly Trp, Pro, Phe, Leu, Ile, Val, Cys, Met; acidic: Asp, Glu; basic: Arg, Lys. The average solvent accessible surface areas for all the CAs is $11,710 \pm 766 \text{ \AA}^2$.

the buffers used in the purification and crystallization of the enzyme. To what extent L4 is specific for Na^+ or can bind other alkali cations remains to be established. To the best of our knowledge, dCA II is the only CA found to have a cation-binding loop.

The noncatalytic additional Zn^{2+} is located at the interface of the two noncrystallographic-symmetry-related molecules (Fig. 5b and 6, which are published as supporting information on the PNAS web site) and is tetrahedrally coordinated by two His-13 residues and two water molecules as shown in Fig. 5b. This Zn^{2+} , and a hydrophobic patch of 567 \AA^2 at the dimer interface, suggested that dCA II assumes a dimeric form also in solution. However, analyses of an extensively dialyzed dCA II by gel-filtration chromatography and atomic-absorption spectroscopy were consistent with dCA II being a monomer containing a single Zn^{2+} (data not shown).

Surface Properties of dCA II Vis-à-Vis Halophilic Proteins. The structure of dCA II was compared with other CA structures also in variable regions that are mostly comprised of loops and turns localized at the protein surface. Table 3 shows that the solvent-accessible surface of dCA II differs from that of the other CAs in possessing a high ratio of acidic over basic amino acid residues resulting from a lowered level of basic residues, primarily lysines. At the same time, the level of acidic residues is kept similar to that of the mesophilic homologs. The selective decrease of Lys content in dCA II not only affects the surface charge but also serves to decrease the surface hydrophobic character, as reported in ref. 6 for halophilic proteins.

The unusual surface amino acid composition of dCA II made it of interest to compare its electrostatic surface potential with that of other CAs (Fig. 2). The predominantly negative surface electrostatic potential of dCA II is strikingly different from the uneven distribution of neutral, negative, and positive potentials characteristic of the other CAs, with the exception of the acidic "back" hemisphere of hCA XII. In this respect, dCA II surface resembles halophilic protein surfaces (1, 3–5, 7, 8). Nonetheless, dCA II differs markedly from halophilic proteins primarily in its ability to fold correctly (19) and to maintain solubility and enzymatic activity at low salt concentration (Tables 1 and 2). Additionally, the far-UV CD and intrinsic fluorescence spectra shown in Fig. 7, which is published as supporting information on the PNAS web site, indicate that the dCA II structure does not vary significantly in response to salinity shifts ranging from 0 to 3.0 M NaCl, thus excluding salt-dependent conformational changes.

In search of a plausible basis for the unusual salt responses of dCA II, the density of charged amino acids on the protein surface was compared with that of mesophilic homologs (Fig. 2) as well

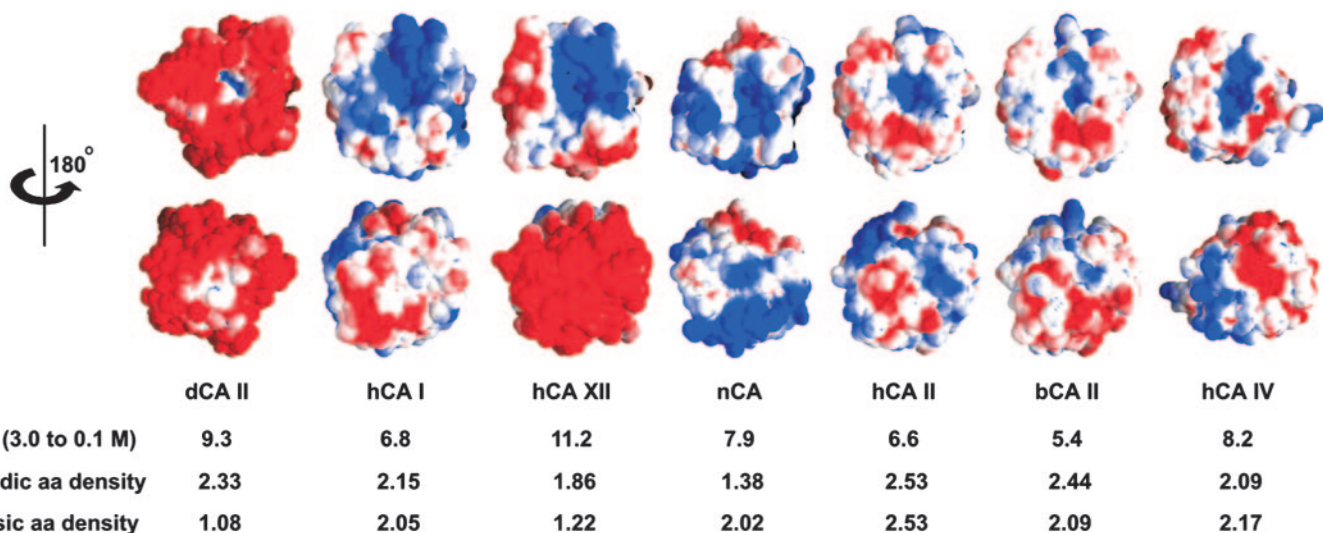


Fig. 2. Electrostatic properties of dCA II and mesophilic CAs. The surface electrostatic potentials were calculated by using GRASP. The structures are graphically depicted looking down the active site cleft (first row) or as the 180° rotated view (second row). The potentials are contoured to -2.5 kT per electron (red) and $+2.5$ kT per electron (blue). The details of the electrostatic free energy (kcal/mol) calculations are presented in *Supporting Text*. The densities of acidic and basic residues per 10^3Å^2 were calculated from the ratio of the number of surface acidic (D and E) or basic (K and R) residues to total accessible surface area.

as with values reported for halophilic proteins (5). The halotolerant dCA II is outstanding among the CA structures compared in its low surface density of basic residues. However, the surface density of 2.33 acidic residues per 10^3Å^2 is similar to that of the mesophilic CAs with the possible exception of the rather basic bacterial nCA. Conversely, 3 crystal structures and 185 homology models of halophilic proteins show an average density of 4.07 acidic residues per 10^3Å^2 as compared with an average of 2.50–2.86 acidic residues per 10^3Å^2 for mesophilic proteins (5), a value close to that observed for dCA II.

The effect of salt on dCA II stability was assessed by solving the nonlinear Poisson–Boltzmann equation for the entire protein molecule at various NaCl concentrations (Fig. 2). The loss of 9.3 kcal/mol in electrostatic free energy of dCA II on lowering the NaCl concentration from 3.0 to 0.1 M is within the range exhibited by the mesophilic CAs with which it was compared. A similar comparison of halophilic and mesophilic ferredoxins transferred from 5.0 to 0.1 M NaCl indicated a free energy loss of 17.3 kcal/mol for the halophilic protein in contrast to a loss of only 3.7 kcal/mol calculated for its mesophilic homolog (37), in keeping with the strong destabilization of halophilic proteins at low salt concentrations.

Active Site Structure. In addition to the need for maintaining the global structure in varying salinities, dCA II should be exceptionally resistant to anion inhibition, because its mesophilic counterparts are normally inhibited by low salt (Tables 1, 2, and 6). However, structural superposition of residues located within $\approx 8 \text{Å}$ from the catalytic Zn^{2+} in dCA II and hCA II shows that these residues are highly conserved and occupy essentially identical positions (the detailed description is presented in *Supporting Text*; see also Fig. 8*b*, which is published as supporting information on the PNAS web site). The catalytic Zn^{2+} of dCA II is coordinated with distorted trigonal bipyramidal geometry to three His residues, a water molecule, and the carboxylate oxygen of an acetate anion, originating in a buffer used during the purification of the enzyme (Fig. 8*a*). Binding of acetate to the active site, previously observed in the structures of hCA II and hCA XII, is considered to mimic the binding of the bicarbonate substrate (35, 38).

In another approach to understand the exceptional tolerance

of dCA II to anion inhibition, we calculated the electrostatic potential at a site adjacent to the catalytic Zn^{2+} . This site referred to as “Br-binding site” is defined by the position occupied by Br^- in the structure of a Br–hCA II complex (22), studied to clarify the mechanism of halide inhibition of CA activity. The calculations (Table 4) reveal a markedly lower positive potential at the Br-binding site of dCA II relative to the other CAs included in the comparison. The lower potential, most probably arising from the negative surface potential of dCA II, is likely to diminish the interaction efficiency of anions, e.g., Cl^- , with the active site, consequently enhancing salt tolerance.

Proposed Structural Basis for dCA II Salt Tolerance. A number of features of dCA II can be considered as potential determinants of salt tolerance. The predominantly negative surface electrostatic potential endows the enzyme with the electrostatic properties that, in analogy to halophilic proteins, can enhance stability and solubility of the protein in high salt. Conversely, the lower surface negative charge density of dCA II, close to that of mesophilic homologs, can enable the protein to fold correctly even at low salt. Long-range electrostatic interactions, probably involving the surface negative charges, lower the positive po-

Table 4. Electrostatic potential at the Br-binding site

CAs	Potential at Br-binding site, kT/e
dCA II	11.0
hCA II	19.9
hCA I	20.0
nCA	20.0
hCA IV	17.5
bCA II	23.3
hCA XII	24.5

The definition and coordinates of the Br-binding site are as described in the text. The coordinates for the various CAs were determined by superimposing the respective structures on the structure of hCA II complexed with Br (Protein Data Bank ID Code 1RAZ) (22). The approximate location of the Br-binding site corresponds to the Zn-bound water (Wat in Fig. 8*a*). The average potential [kT per electron (e)] for 720 points within 0.2Å around the Br-binding coordinate was calculated as described in *Materials and Methods*.

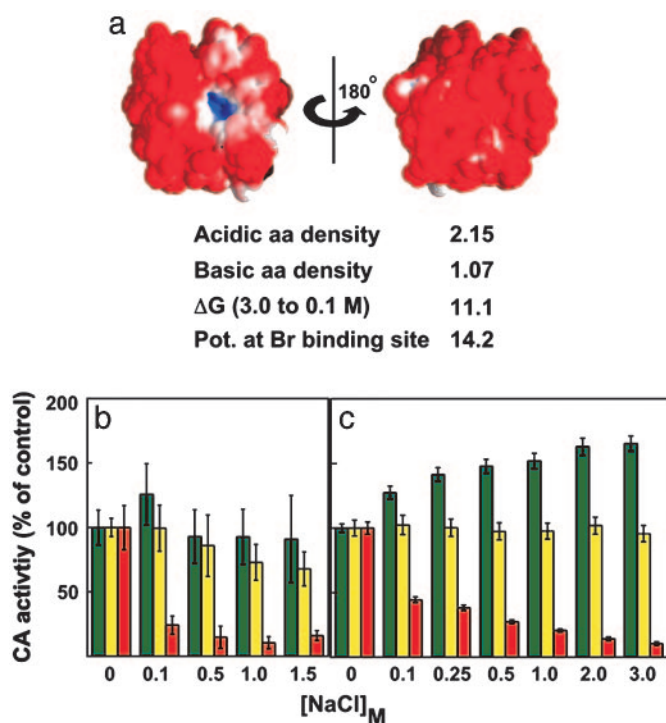


Fig. 3. Electrostatic properties and effect of salt on enzymatic activity of mCA XIV. (a) The surface electrostatic potentials, the decrease in electrostatic free energy on transfer from 3.0 to 0.1 M NaCl, and surface density of acidic and basic residues are as described in Fig. 2. (b and c) Assays of CO₂ hydration activity (b) and ester hydrolysis activity (c) of dCA II (green), mCA XIV (yellow), or hCA I (red) were performed as described in *Materials and Methods*. Controls indicate enzyme activity in the absence of salt. For esterase activity, 0.5 mM *p*-nitrophenyl acetate was used as substrate. Pot, electrostatic potential.

tential at the Br-binding site, thus rendering dCA II less sensitive to Cl⁻ inhibition. Furthermore, electrostatic repulsion by the negative surface charges, particularly those close to the active site entrance, might hinder the approach of inhibitory anions to the active site. In addition to its electrostatic properties, the two extended surface α -helices and the Na-binding loop in dCA II probably serve as stabilizing factors in high salt. Extended helices have been implicated in the stability of thermophilic and halophilic proteins (4, 39). Specific bindings of ions such as K⁺, Na⁺, or Cl⁻ have been implied in stabilizing intersubunit or crystal packing interfaces in several halophilic proteins (4, 9, 10). Nonetheless, a Na-binding loop as found in dCA II has not been reported yet in halophilic proteins.

The critical role of the electrostatic properties in the salt tolerance of the algal dCA II is strongly supported by the ability of these properties to predict the unexpected halotolerance of a phylogenetically remote homolog, the murine CA XIV. The predominantly negative surface potential of the extracellular catalytic domain of CA XIV (Fig. 3a), based on its recently determined crystal structure (40), bears a strong resemblance to that of dCA II (see Fig. 2). This initially observed similarity was subsequently extended to several other characteristic properties of dCA II, i.e., the low density of surface basic amino acid residues relative to acidic residues; the relatively small change in electrostatic free energy accompanying a transition from high to low salinity; and the lowered positive electrostatic potential, albeit to a lower extent than in dCA II, at the Br-binding site (see Figs. 2 and 3a). The power of these properties to predict the salt tolerance of mCA XIV was unequivocally demonstrated in assays of CO₂ hydration (Fig. 3b) and esterase (Fig. 3c) activities in the presence of 0–3.0 M NaCl. Shown together with corre-

sponding activities of dCA II and hCA I, the results demonstrate the outstanding salt tolerance of mCA XIV, albeit to a slightly lower extent than that of dCA II or dCA I (18). This difference could be related to the absence in mCA XIV of elements such as the extended helices and the Na-binding loop as well as the slightly higher positive electrostatic potential compared with dCA II at the Br-binding site of mCA XIV.

Discussion

Similarly to the dCA I described in refs. 32 and 33, the salt-inducible single-domain dCA II is thought to act by converting bicarbonate, the major source of inorganic carbon available to *Dunaliella*, to CO₂ that diffuses readily into the cells. As we have predicted (18), the enzymatic assays of dCA II conducted in low to multimolar NaCl concentrations indeed demonstrated its unusual salt tolerance.

To the best of our knowledge, the dCA II crystal structure is the first reported 3D structure of a *Dunaliella* protein (www.ncbi.nlm.nih.gov/Taxonomy) as well as of a bona fide halotolerant protein from any source. Spectral analyses of dCA II in solution indicated that it does not undergo meaningful conformational transitions as a function of salt concentration. Hence, the structure determined at low salt, as described here, should be valid for a broad range of salinities.

Extensive studies of mammalian α -type CAs, emanating from their physiological and medical interest, included the determination of numerous 3D structures of free and inhibitor-complexed enzymes. Thus, the halotolerant dCA II structure could be critically viewed against the landscape of a wealth of structures of mesophilic homologs. Shared structural and functional properties of halophilic proteins provided another frame of reference because no halophilic CA has been reported yet.

The basis proposed for the salt tolerance of dCA II considers unique secondary structure elements likely to enhance its stability in high salt but primarily stresses the contribution of the negative electrostatic surface potential. The electrostatic interactions considered here could be partly akin to mechanisms proposed for modulation of enzymatic activity by “steering” of substrates toward the active site (41–43) or modification of interaction potentials within the active site (44).

The unanticipated discovery of the exceptional halotolerance of mCA XIV upholds the predictions drawn from the dCA II structure and furthermore raises intriguing questions regarding the functional significance of the halotolerance of a mammalian homolog. CA XIV has been identified in several tissues including brain, liver, and kidney. In the kidney, CA XIV has been localized to the proximal convoluted tubule (40, 45, 46), particularly in the apical plasma membrane, i.e., brush border (46), of the S1 and S2 segments, where $\approx 90\%$ of the bicarbonate in the renal filtrate is reabsorbed into the blood. In this process, protons secreted into the lumen, mainly by the brush border Na⁺/H⁺ exchanger, protonate the luminal bicarbonate to carbonic acid that is dehydrated by a membrane-associated CA(s) to CO₂ that easily permeates the brush border membranes. Within the cells, the reverse series of events, catalyzed by a cytoplasmic CA, generates bicarbonate that is reabsorbed into the blood across the basolateral membrane. Normally, the lumen pH falls from 7.4 at the glomerulus to ≈ 6.7 along the length of the proximal tubule, as the bicarbonate is reabsorbed and the buffer capacity of the luminal fluid decreases. It is conceivable that the local pH at the brush border, the site of proton secretion, is even lower than that in the lumen itself, due to the restricted diffusion of protons or bicarbonate.

The earlier view ascribing the membrane-associated luminal CA activity solely to CA IV has been revised upon the identification of CA XIV as a luminal CA localized mostly at distinct sites from CA IV (46). The question whether CA IV and CA XIV at the proximal convoluted tubule are functionally redun-

dant or physiologically distinct can now be considered in view of the unexpected halotolerance of CA XIV. Because no osmotic build-up is known to take place at the proximal convoluted tubule sections where the enzyme is localized, we considered the possibility that acidification, by the mechanism proposed above, was the critical environmental factor underlying the salt adaptation of CA XIV. As shown in our present and earlier studies, dCA II as well as dCA I remain almost resistant to anion inhibition even at a pH of ≈ 5.5 (18), in contrast to the large increase in anion sensitivity generally exhibited by mammalian homologs. For example, the K_i for chloride inhibition of bicarbonate dehydration by hCA IV at pH 5.5 is 36 mM (47), a value lower than the physiological concentration of chloride. In contrast, mCA XIV exhibited at pH 5.6 an IC_{50} of ≈ 250 mM for chloride inhibition (data not shown), a level significantly higher than that reported for hCA IV, albeit lower than that of the algal CAs (18). Thus, CA XIV should remain active under conditions that limit the activity of CA IV. The specific significance of CA IV to bicarbonate absorption in the proximal convoluted tubule still remains to be elucidated.

In conclusion, our studies shed light on the molecular adaptations of α -type carbonic anhydrases that radically enhance

their salt tolerance while conserving the active site architecture and typical global fold except for modifications that potentially increase the overall stability of the protein. Surface electrostatic properties intermediate between those of halophilic and mesophilic proteins play an essential role in the halotolerance of dCA II. Whether other halotolerant proteins share the surface electrostatic characteristics of dCA II must await further structure determinations. The large difference in anion sensitivity emerging from the disparate electrostatic properties of CA XIV and other mammalian isozymes has far-reaching implications for isozyme-selective drug design.

We thank Prof. W. S. Sly for kindly providing the affinity-purified mCA XIV, Prof. S. J. D. Karlish for helpful advice and ideas concerning kidney physiology, and Prof. B. Honig for critical suggestions concerning electrostatic calculations. The structure was determined in collaboration with the Israel Structural Proteomics Center. This work was supported by the Israel Ministry of Science and Technology, European Commission Structural Proteomics Project Grant QL2-CT-2002-00988, and the Divadol Foundation. A.Z. was supported by Nature Beta Technologies (Eilat, Israel) and Nikken-Sohonsha Corp. (Gifu, Japan). J.L.S. is the Morton and Gladys Pickman Professor of Structural Biology.

- Madern, D., Ebel, C. & Zaccai, G. (2000) *Extremophiles* **4**, 91–98.
- Mevarech, M., Frolow, F. & Gloss, L. (2000) *Biophys. Chem.* **86**, 155–164.
- Dym, O., Mevarech, M. & Sussman, J. L. (1994) *Science* **267**, 1344–1346.
- Frolow, F., Harel, M., Sussman, J. L., Mevarech, M. & Shoham, M. (1996) *Nat. Struct. Biol.* **3**, 452–458.
- Bieger, B., Essen, L. O. & Oesterhelt, D. (2003) *Structure (London)* **11**, 375–385.
- Britton, K., Stillman, T., Yip, K., Forterre, F., Engel, P. & Rice, D. (1998) *J. Biol. Chem.* **273**, 9023–9030.
- Ebel, C., Costenaro, L., Pascu, M., Faou, P., Kernel, B., Proust-De Martin, F. & Zaccai, G. (2002) *Biochemistry* **41**, 13234–13244.
- Costenaro, L., Zaccai, G. & Ebel, C. (2002) *Biochemistry* **41**, 13245–13252.
- Richard, S. B., Madern, D., Garcin, E. & Zaccai, G. (2000) *Biochemistry* **39**, 992–1000.
- Irimia, A., Ebel, C., Madern, D., Richard, S. B., Cosenza, L. W., Zaccai, G., Vellieux, F. M., Costenaro, L., Pascu, M., Faou, P., et al. (2003) *J. Mol. Biol.* **326**, 859–873.
- Deutch, C. E. (2002) *Lett. Appl. Microbiol.* **35**, 78–84.
- Polosina, Y. Y., Zamyatkin, D. F., Kostyukova, A. S., Filimonov, V. V. & Fedorov, O. V. (2002) *Extremophiles* **6**, 135–142.
- Wejse, P. L., Ingvorsen, K. & Mortensen, K. K. (2003) *Extremophiles* **7**, 423–431.
- Yoshimune, K., Yamashita, R., Masuo, N., Wakayama, M. & Moriguchi, M. (2004) *Extremophiles* **8**, 441–446.
- Madern, D. & Zaccai, G. (2004) *Biochimie* **86**, 295–303.
- Ahmad, A., Akhtar, M. S. & Bhakuni, V. (2001) *Biochemistry* **40**, 1945–1955.
- Avron, M. (1986) *Trends Biochem. Sci.* **11**, 5–6.
- Bageshwar, U. K., Premkumar, L., Gokhman, I., Savchenko, T., Sussman, J. L. & Zamir, A. (2004) *Protein Eng. Des. Sel.* **17**, 191–200.
- Premkumar, L., Greenblatt, H. M., Bageshwar, U. K., Savchenko, T., Gokhman, I., Zamir, A. & Sussman, J. L. (2003) *Acta Crystallogr. D* **59**, 1084–1086.
- Lindskog, S. & Silverman, D. N. (2000) in *The Carbonic Anhydrases: New Horizons*, eds. Chegwidden, W. R., Carter, N. D. & Edwards, Y. H. (Birkhauser, Basel), pp. 175–195.
- Liljas, A., Hakansson, K., Jonsson, B. H. & Xue, Y. (1994) *Eur. J. Biochem.* **219**, 1–10.
- Jonsson, B. M., Hakansson, K. & Liljas, A. (1993) *FEBS Lett.* **322**, 186–190.
- Premkumar, L., Bageshwar, U. K., Gokhman, I., Zamir, A. & Sussman, J. L. (2003) *Protein Expression Purif.* **28**, 151–157.
- Otwinowski, Z. & Minor, W. (1997) *Methods Enzymol.* **276**, 307–326.
- Brunger, A. T., Adams, P. D., Clore, G. M., DeLano, W. L., Gros, P., Grosse-Kunstleve, R. W., Jiang, J. S., Kuszewski, J., Nilges, M., Pannu, N. S., et al. (1998) *Acta Crystallogr. D* **54**, 905–921.
- McRee, D. E. (1999) *J. Struct. Biol.* **125**, 156–165.
- Kabsch, W. & Sander, C. (1983) *Biopolymers* **22**, 2577–2637.
- Kleywegt, G. J. & Jones, T. A. (1994) *ESF/CCP4 Newsletter* **31**, 9–14.
- Guex, N. & Peitsch, M. C. (1997) *Electrophoresis* **18**, 2714–2723.
- Nicholls, A., Sharp, K. A. & Honig, B. (1991) *Proteins* **11**, 281–296.
- Honig, B. & Nicholls, A. (1995) *Science* **268**, 1144–1149.
- Fisher, M., Pick, U. & Zamir, A. (1994) *Plant Physiol.* **106**, 1359–1365.
- Fisher, M., Gokhman, I., Pick, U. & Zamir, A. (1996) *J. Biol. Chem.* **271**, 17718–17723.
- Stams, T., Nair, S. K., Okuyama, T., Waheed, A., Sly, W. S. & Christianson, D. W. (1996) *Proc. Natl. Acad. Sci. USA* **93**, 13589–13594.
- Whittington, D. A., Waheed, A., Ulmasov, B., Shah, G. N., Grubb, J. H., Sly, W. S. & Christianson, D. W. (2001) *Proc. Natl. Acad. Sci. USA* **98**, 9545–9550.
- Pineda, A. O., Carrell, C. J., Bush, L. A., Prasad, S., Caccia, S., Chen, Z. W., Mathews, F. S. & Di Cera, E. (2004) *J. Biol. Chem.* **279**, 31842–31853.
- Elcock, A. H. & McCammon, J. A. (1998) *J. Mol. Biol.* **280**, 731–748.
- Hakansson, K. (1994) *Acta Crystallogr. D* **50**, 101–104.
- Chakravarty, S. & Varadarajan, R. (2002) *Biochemistry* **41**, 8152–8161.
- Whittington, D. A., Grubb, J. H., Waheed, A., Shah, G. N., Sly, W. S. & Christianson, D. W. (2004) *J. Biol. Chem.* **279**, 7223–7228.
- Getzoff, E. D., Tainer, J. A., Weiner, P. K., Kollman, P. A., Richardson, J. S. & Richardson, D. C. (1983) *Nature* **306**, 287–290.
- Ripoll, D. R., Faerman, C. H., Axelsen, P. H., Silman, I. & Sussman, J. L. (1993) *Proc. Natl. Acad. Sci. USA* **90**, 5128–5132.
- Stroppolo, M. E., Falconi, M., Caccuri, A. M. & Desideri, A. (2001) *Cell. Mol. Life Sci.* **58**, 1451–1460.
- Jackson, S. E. & Fersht, A. R. (1993) *Biochemistry* **32**, 13909–13916.
- Parkkila, S., Parkkila, A. K., Rajaniemi, H., Shah, G. N., Grubb, J. H., Waheed, A. & Sly, W. S. (2001) *Proc. Natl. Acad. Sci. USA* **98**, 1918–1923.
- Kaunisto, K., Parkkila, S., Rajaniemi, H., Waheed, A., Grubb, J. & Sly, W. S. (2002) *Kidney Int.* **61**, 2111–2118.
- Baird, T. T., Waheed, A., Okuyama, T., Sly, W. S. & Fierke, C. A. (1997) *Biochemistry* **36**, 2669–2678.